

## TN 376 Brownlee team cruise report

### 1. Rationale and approaches

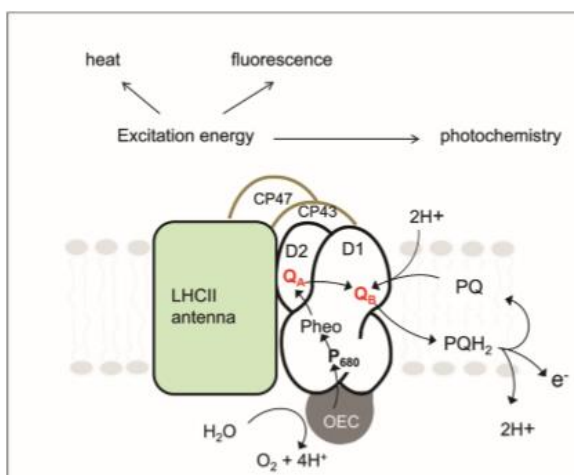
We have applied photophysiological and molecular genetic approaches in order to better understand the drivers and constraints on phytoplankton abundance, community composition and productivity. We have used Pulse Amplitude Modulated (PAM) fluorimetry of freshly isolated samples together with sub-samples from incubation experiments.

### 2. Objectives

- To determine the spatial distributions (surface, depth profiles) of parameters of photosynthetic efficiency to address the following:
- Identify correlations with environmental factors – salinity, temperature, nutrients, carbonate chemistry.
- To uncover any relationships between particular phytoplankton groups major species composition
- Use this information, broadly defined as photosynthetic efficiency parameters, together with more detailed analysis from eDNA and eRNA samples and EM preparations to gain indications of efficient growth as well as physiological stress arising from nutrient deficiency and/or potential biotic interactions (competition, chemical warfare).

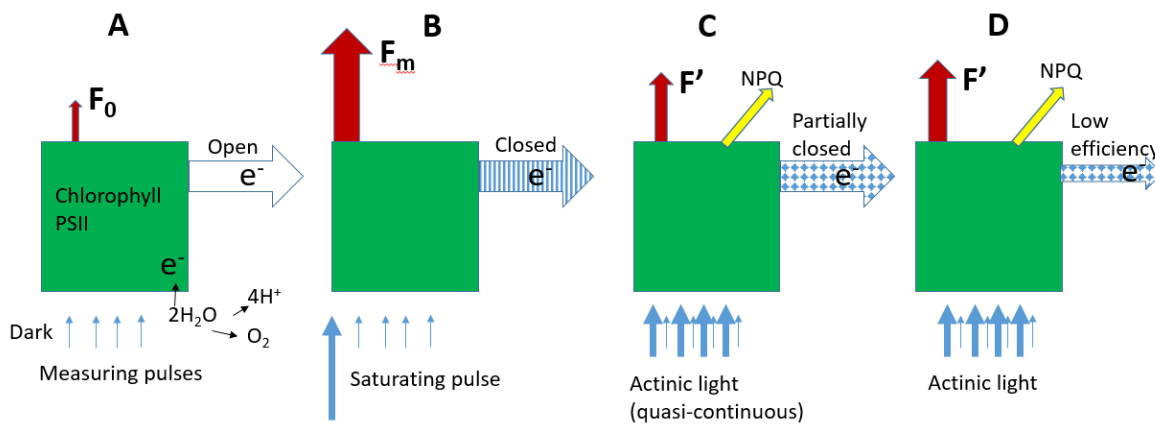
### 3. PAM fluorimetry

PAM fluorimetry is a widely used method for rapid assessment of the physiological state of the photosynthetic machinery in plants. The approach is based on measurement of chlorophyll fluorescence of photosystem II (PSII) as an indicator of **the efficiency with which light absorbed by the photosynthetic machinery and converted into useful work in the form of electron transport in the chloroplast thylakoid membrane**. The electron transport chains are ultimately responsible for providing the chemical energy for photosynthetic carbon fixation. Figure 1 shows a simplistic scheme of the components of chlorophyll PSII system (see e.g. Murchie & Lawson (2003) for a more detailed accessible guide to PAM fluorimetry).



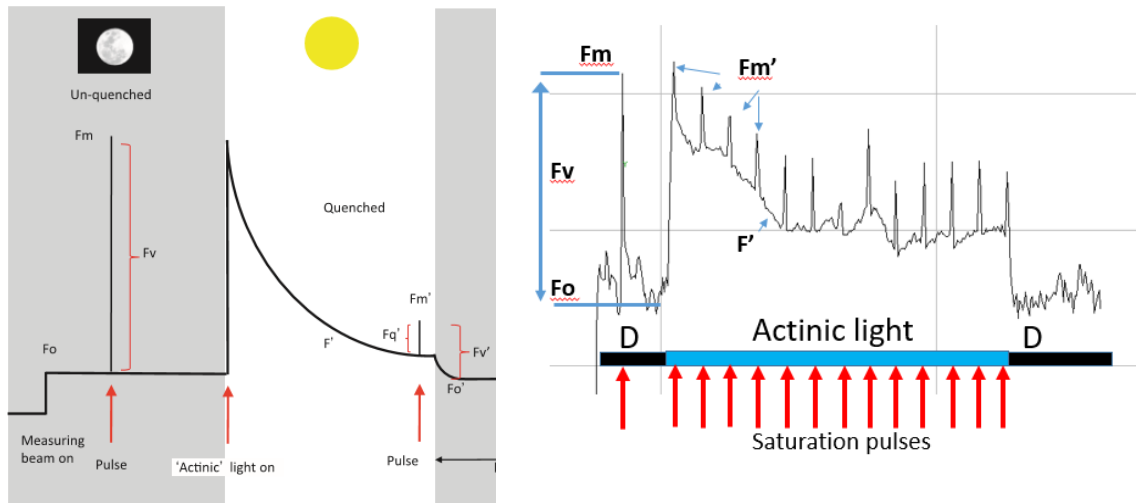
**Figure 1.** Energy conversion by PSII. Light absorbed by the chlorophyll light harvesting complex (LHCII) drives the hydrolysis of water into O<sub>2</sub>, H<sup>+</sup> and electrons. Transfer of electrons through the components of the electron transport chain in the thylakoid membrane of the chloroplast energises the photosynthetic machinery, eventually leading to the fixation of carbon from CO<sub>2</sub>. Excess light energy absorbed by chlorophyll/PSII is lost as fluorescence or through chemical quenching and heat (non-photochemical quenching, NPQ). From Murchie & Lawson (2013)

Figure 2 provides a simplistic cartoon to illustrate how chlorophyll fluorescence varies under the different light pulse protocols used in PAM fluorimetry. The values of chlorophyll fluorescence ( $F_0$ ,  $F_m$  and  $F'$ ) are used to calculate the efficiency parameters.



**Figure 2.** Illustration of how chlorophyll fluorescence measurements are made and used to assess photosynthetic efficiency in PAM fluorimetry. Light energy absorbed by chlorophyll can either be converted into electrons or lost as fluorescence or heat (NPQ). Photosynthetic efficiency is a measure of the efficiency of conversion of incident light into useful electron transport. **A:** In dark-adapted cells, the photosynthetic reaction centres, through which electrons are transferred, are open. Short, low amplitude measuring pulses of light produce low levels of resting fluorescence ( $F_0$ ). **B:** A strong pulse of light saturates the electron transport chain and leads to the closure of photosynthetic reaction centres. Electrons produced by chlorophyll/PSII cannot be efficiently transferred resulting in corresponding increased fluorescence, measured immediately after the saturating light pulse ( $F_m$ ). **C:** Measuring light pulses given in rapid alternation with actinic light monitor the fluorescence arising from the partial closure of reaction centres as electrons move through them in the light-activated photosynthesising state. Decreases in the fluorescence signal (quenching) may occur as non-photochemical quenching (NPQ) reactions are activated. **D:** Cells in which the electron transport chain or carbon fixation are compromised in some way (e.g. through nutrient deficiency) may show increased fluorescence due to the electron transport chain working less efficiently. By monitoring the ratio of fluorescence values after different light pulses, **by measuring values of  $F_0$ ,  $F_m$  and  $F'$  during different illumination regimes**, the efficiency by which absorbed light is converted into electron transport can be calculated.

Figure 3 provides a theoretical and actual experimental quench curve used to obtain the values of chlorophyll fluorescence. Experimental measurements were made with a PAM fluorimeter (Water PAM, Walz, Germany) with 3 ml cuvette samples that were dark-adapted for >30 minutes prior to analysis.



**Figure 3. Left:** Schematic of a PAM quench curve, showing the measurement of  $F_o$ ,  $F_m$  after the initial saturating pulse and  $F'$  values during the onset of actinic light illumination. **Right:** Representative quench curve obtained from a cruise sample (Station 43, 5m depth). The peaks during the actinic light period are in response to additional saturating pulses that are used to measure effective photosynthetic quantum yield ( $Y_{II}$ ) and NPQ. NPQ values are calculated when quenching reaches a steady state at the end of the quench period (normally around 5 minutes).

The following key photosynthetic parameters were calculated from values of  $F_o$ ,  $F_m$ ,  $F'_m$  and  $F'$ :

- Maximum photosynthetic efficiency/capacity of dark –adapted cells:

$$F_v/F_m = (F_m - F_o)/F_m$$

- Effective photochemical quantum yield of PSII (photosynthetic efficiency in light conditions):

$$Y_{II} = (F'_m - F')/F'_m$$

- Electron transfer rate (ETR) at a given irradiance value = proportion of photons at a given light intensity that are converted into useful energy.

$$ETR = Y_{II} \times PAR$$

- Non-photochemical quenching

$$NPQ = F_m/F'_m - 1$$

- Rapid light curves were also carried out to acquire ETR values at different irradiance values, providing information on initial slope ( $\alpha$ ),  $ETR_{max}$  at saturating irradiance and photoinhibition.

#### 4. Preliminary analyses

**4.1. Meander surveys.** Figures 4 and 5 show surface underway photosynthetic parameters ( $F_o$ ,  $F_v/F_m$ , ETR) along VPR tracks during the first meander survey, together with salinity, temperature and  $bb_{prime}$  distributions. Preliminary examination reveals generally low values of  $F_o$  in regions of high salinity and temperature. In contrast,  $F_v/F_m$  values were generally higher in low salinity regions.

High Fv/Fm values were also observed in high bbprime and higher temperature regions. ETR values showed less distinct correlations though they more closely matched Fv/Fm values in survey 1. ETR values show a good correlation with bbprime. Figures 6 and 7 show Fo, Fv/Fm and ETR values from surface CTD samples from the meander surveys 1 and 2. Fo values again showed an inverse relation with salinity and temperature. Fv/Fm values correlated positively with temperature and salinity (cf .Figs 4 and 5).

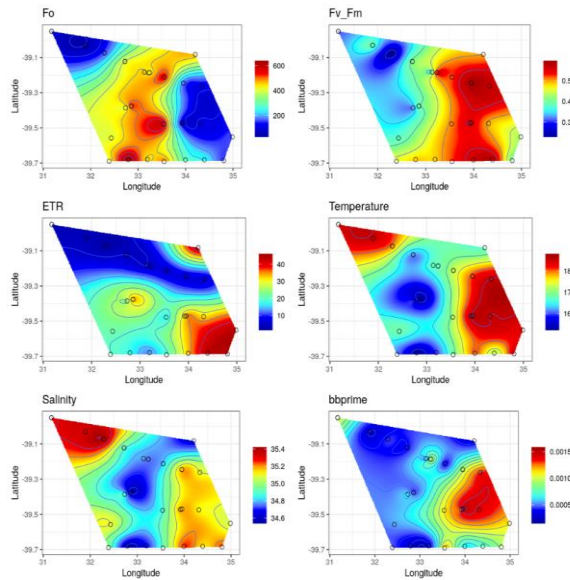


**Fig 4.** Meander VPR survey 1 Underway samples

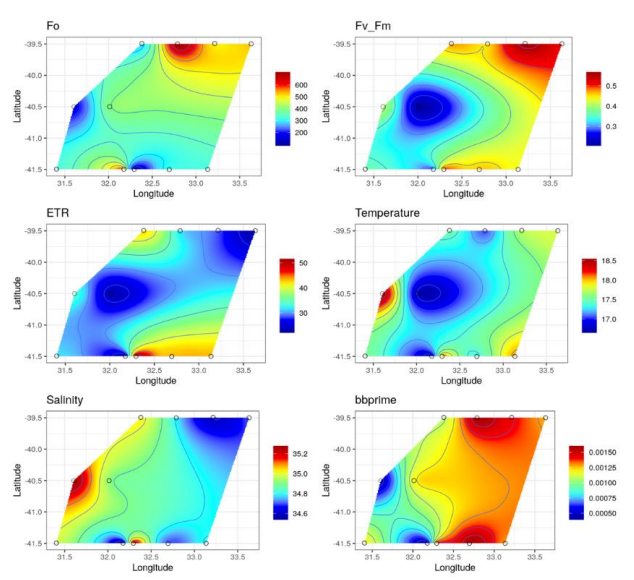


**Fig 5.** Meander VPR survey 2 Underway samples

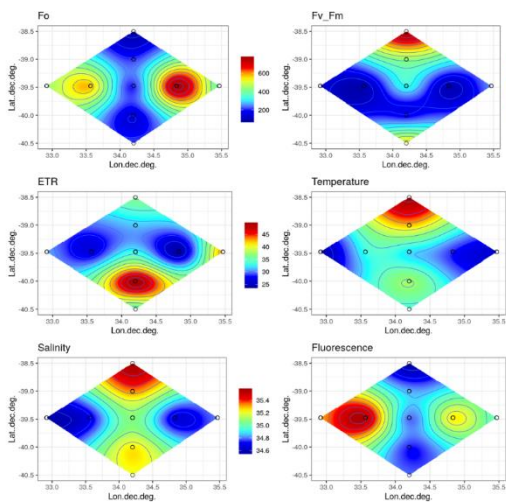


**Fig. 6.** CTD surface features: Meander survey 1 (CTD 8-17)

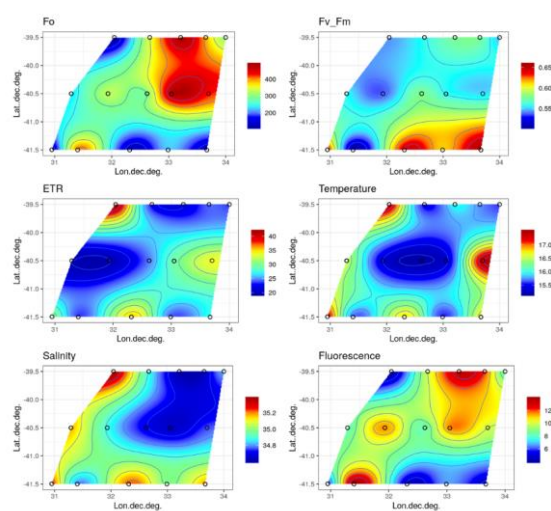


**Fig. 7.** CTD surface features: Meander survey 2 (CTD 18-25)

Figs 7-10 show summary depth profiles for Fo, Fv/Fm and ETR in relation to temperature,

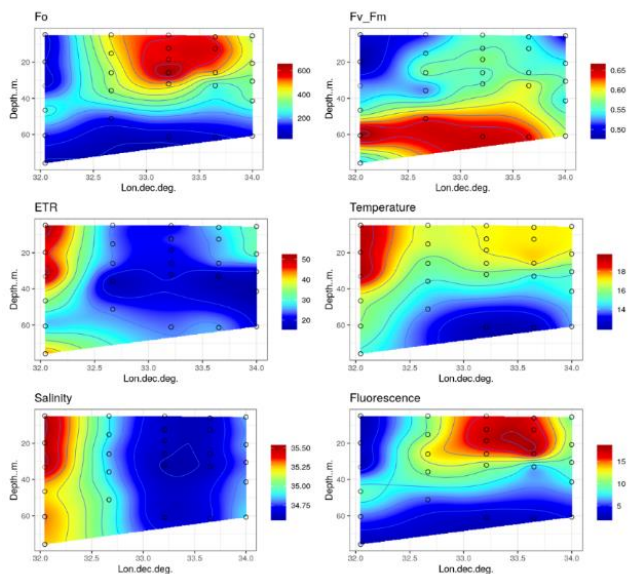


**Fig. 8.** CTD depth profile Meander North transect (CTDs 44-52)

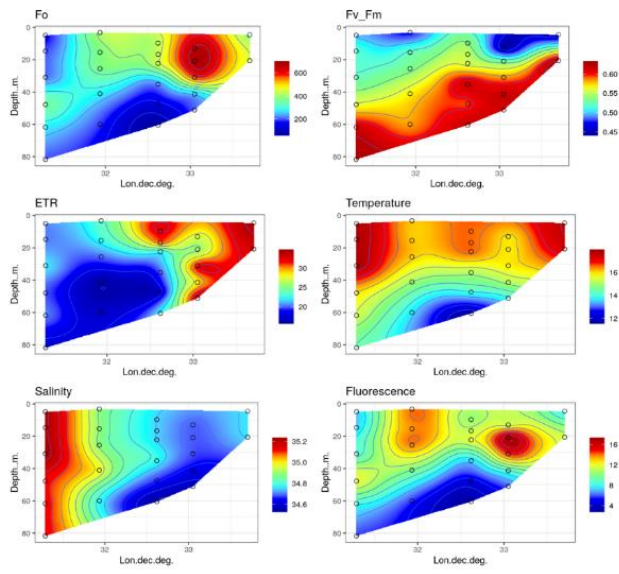


**Fig. 9.** CTD Depth profile Meander Centre transect (CTDs 35-42)

salinity and total chlorophyll fluorescence for

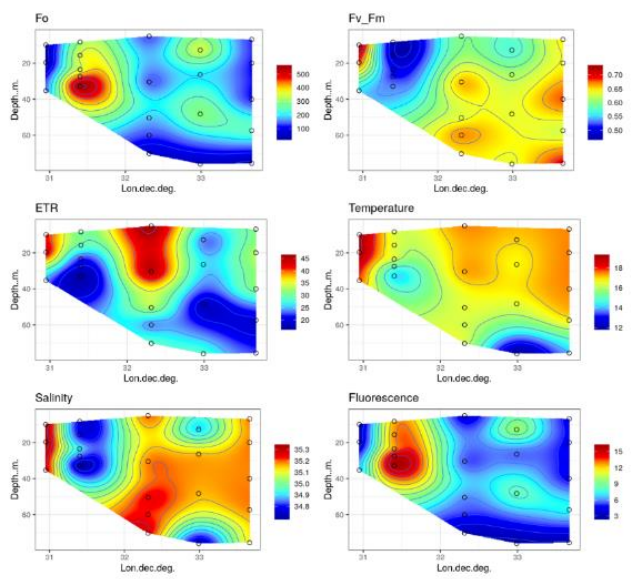


**Fig.10.** CTD Depth profile Meander Southern transect (CTDs 26-34)

North, Central and Southern transects during the second meander survey. In all profiles there is a clear relationship between Fo values and total chlorophyll fluorescence. Fo values tended to correlate negatively with salinity and Fv/Fm. Fv/Fm values showed negative correlations with temperature and Fo/fluorescence and in the Southern transect showed an apparent positive correlation with temperature.

Spearman correlations derived from all Fo, Fv/Fm and ETR measurements are shown in Fig 11. Overall, Fo showed significant negative correlation with salinity and positive correlation with total chlorophyll. Fv/Fm showed an overall positive correlation with salinity and negative correlation with fluorescence. ETR was strongly correlated with temperature, salinity and fluorescence. In addition ETR showed a strong correlation with time of sample collection, showing strongest peaks in samples collected in mornings. Examples of Spearman correlations

for Fo and Fv/Fv are shown in Fig. 10. Further analysis is ongoing. For example the apparent relationship between bbprime and Fo and Fv/Fm is not apparent in the Spearman correlations from all samples, suggesting location-specific relations that may reward further investigation.

## Fv\_Fm

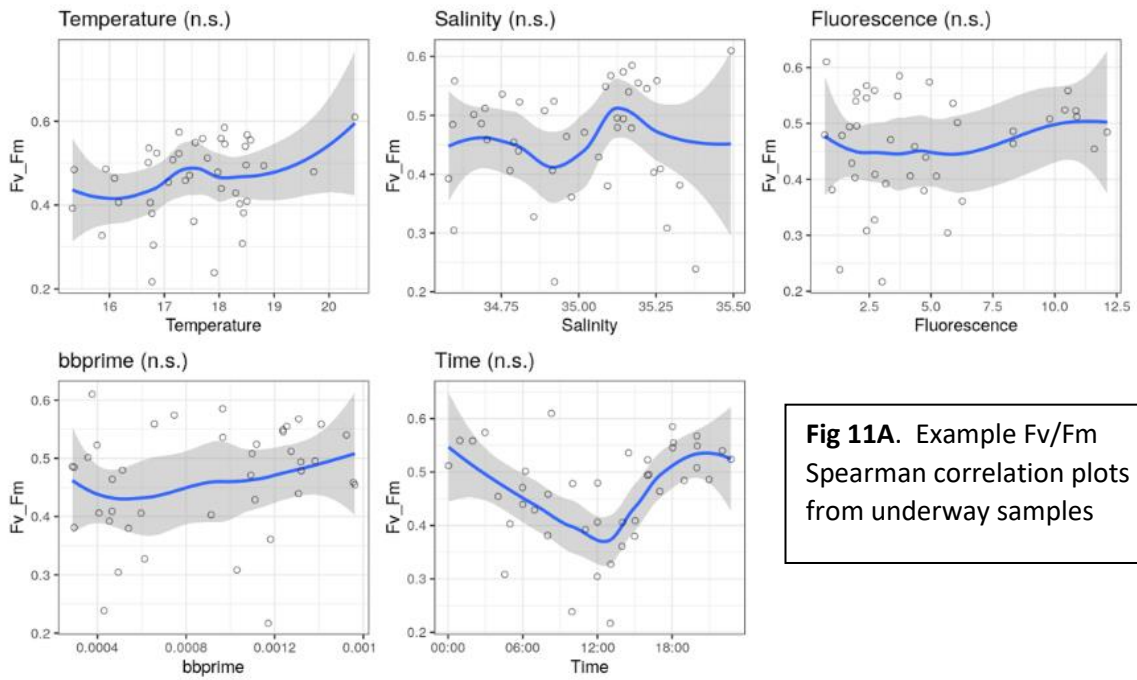


**Fig 11A.** Example Fv/Fm Spearman correlation plots from underway samples

## Fv\_Fm

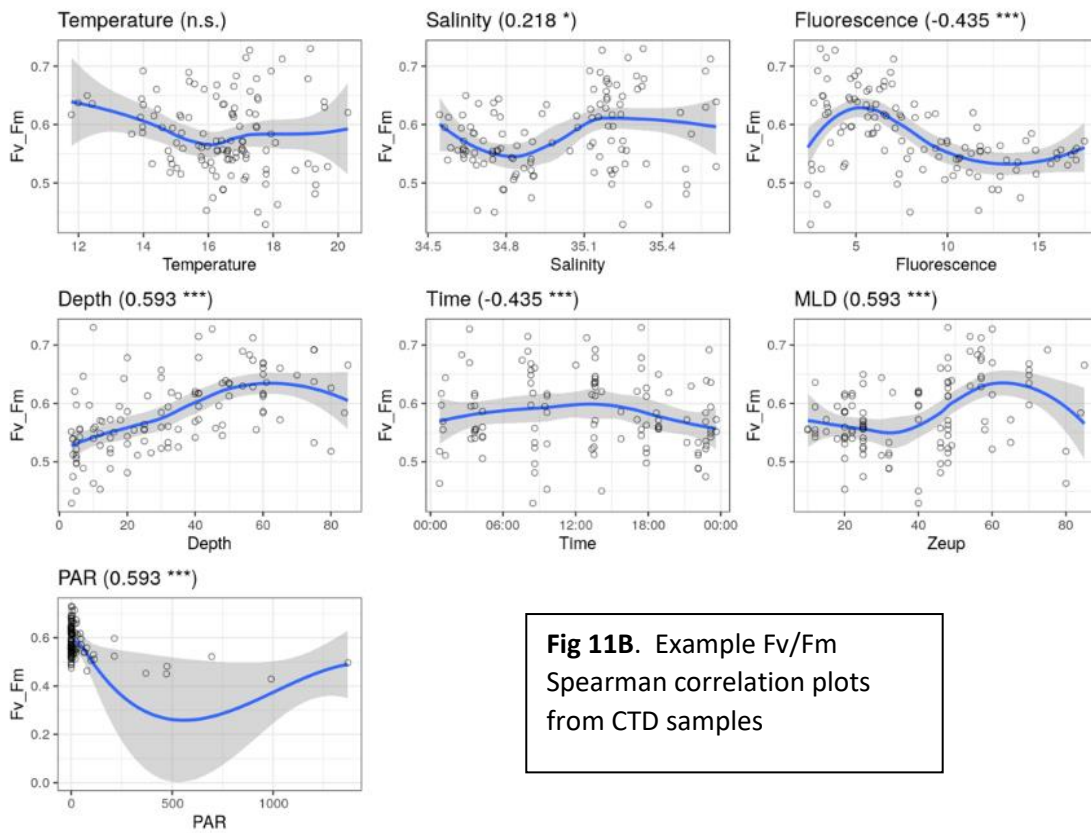


**Fig 11B.** Example Fv/Fm Spearman correlation plots from CTD samples

**4.2. Eddy surveys.** Plots of eddy surveys 1 and 2 are under construction. Fig. 12 shows surface underway values of Fo, Fv/Fm and ETR in relation to temperature, salinity and fluorescence.

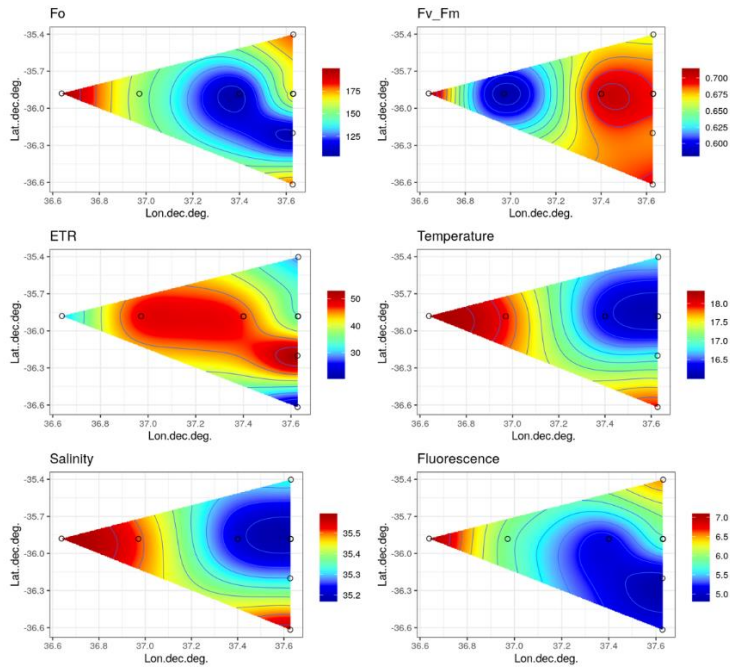


**Fig. 12.** Surface plots of F0, Fv/Fm and ETR for eddy survey 1.

Further analysis of this feature is ongoing.

### 4.3 PAM microscopy

Analysis of single cell chlorophyll fluorescence was applied using similar PAM protocols to the above PAM fluorimeter measurements. The PAM microscope (PSI, Cz) allows images of  $F_o$ ,  $F_m$ ,  $F'_m$  and  $F'$  by using LED arrays to provide measuring pulses, saturating pulses and actinic light. Under rough weather conditions it was only possible to obtain  $F_v/F_m$  values due to focus drift associated with vertical movements of the ship. The microscope allowed acquisition of bright field and polarized light images to identify individual phytoplankton cells and calcifying coccolithophores. Cells were allowed to settle in darkness for >1 hour before gentle transfer to the microscope imaging chamber, which comprised a glass-bottomed dish and X 20 or X40 Zeiss water immersion objectives. The dish was mounted on a temperature controlled perfusion cell, which allowed cells to be maintained at the precise collection temperature. All manipulations were carried out in darkness. Bright field images were obtained using far red light, which does not activate the PSII reaction centres. Fig 13 shows a representative set of images from CTD #50 surface sample, along with  $F_v/F_m$  values of individual coccolithophore and non-coccolithophore (mainly dinoflagellates and small flagellates) cells (see TGT microscopy log.xls for all CTD and underway samples).

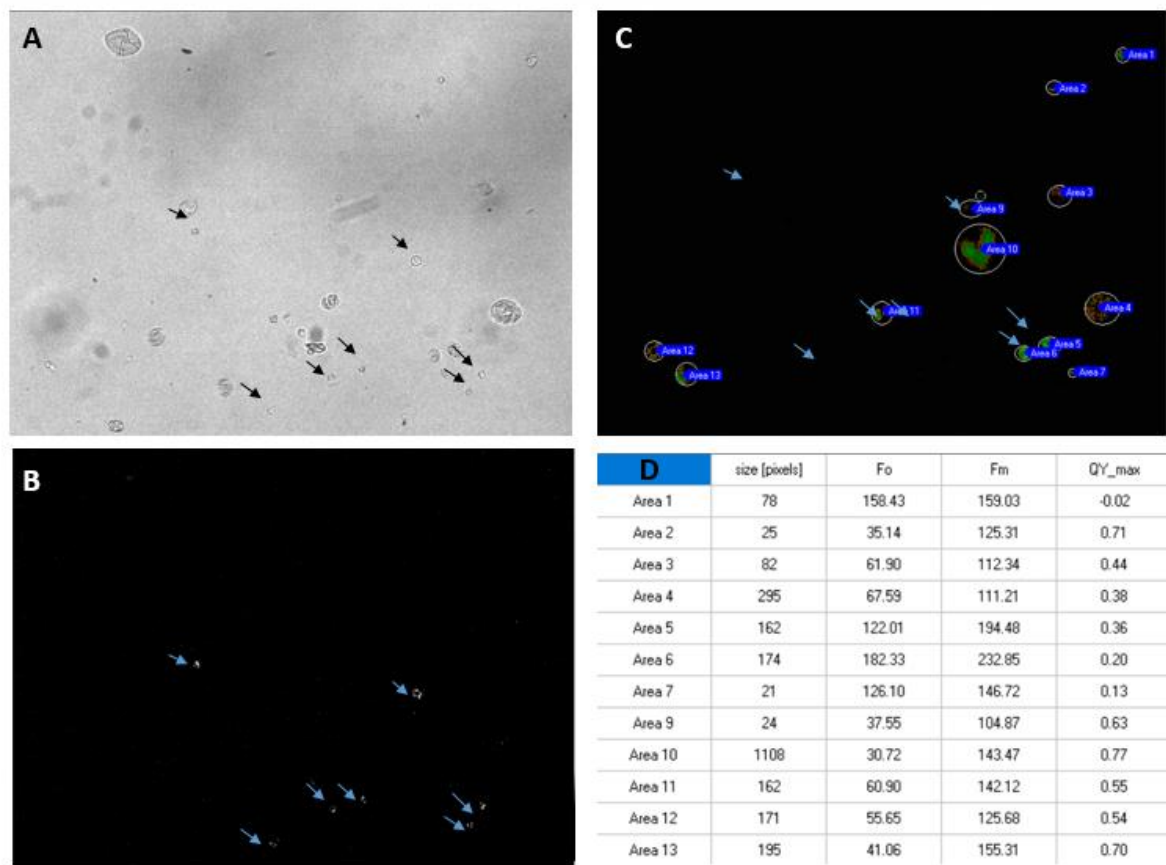


**Fig. 13.** **A:** Bright field image of a mixed phytoplankton sample (CTD 50). Arrows correspond to calcified cells revealed by cross polarised light (**B**). **C:**  $F_v/F_m$  image showing ROIs of cells selected for quantification. **D:**  $F_v/F_m$  (QY) values of cells identified in (**C**).

### ***PAM microscopy key findings:***

- Approximately 175 individual underway or CDT samples, representing >250 individual cells were analysed using PAM microscopy. This pilot study demonstrates the applicability of PAM microscopy on a research vessel. Issues related to vibration were minimal, though slower vertical pitch and roll ship movements limited the application of longer term quench curves. The study focussed on obtaining a dataset of Fv/Fm values.
- The majority of samples comprised mixed populations of coccolithophores and dinoflagellates. The precise proportions of different phytoplankton classes awaits further cell count analyses. While *Emiliana huxleyi* was the most frequently occurring coccolithophore, many samples were notable for the apparent diversity of coccolithophore species.
- Preliminary analysis indicates that mean Fv/Fm values reflect the average values obtained with PAM fluorimetry. However, the single cell analyses have revealed an unexpectedly high variability in single cell Fv/Fm values (e.g. Fig 12 D, with values ranging from <0.2 to >0.7).
- So far, no clear differences have been seen in the average Fv/Fm values of different phytoplankton types, though substantial further analysis is needed to investigate this in more detail.

### ***Questions to address:***

- Can we detect differences in the average Fv/Fm for different phytoplankton groups within a population
- Do the PAM microscopy measurements agree with the PAM fluorimetry?
- Is there greater variability within and between different phytoplankton groups and do any differences in variability in Fv/Fm inform whether particular groups are better adapted to the current conditions?

The PAM fluorimeter measures total population fluorescence parameters, which includes the cyanobacterial signal. Cyanobacteria are excluded from the PAM microscopy measurements, being too small to resolve individual cells. However, cyanobacteria have been observed in significant numbers in fixed slide preparations. Can any differences in PAM fluorimetry and PAM microscopy reflect the contribution of cyanobacteria to the fluorescence properties, and potentially productivity of the population.

#### **4.4 Deck incubation experiments**

Fluorescence parameters were measured from 4 deck incubation experiments, carried out on surface samples from both the meander and eddy features. Incubations were sampled daily for the course of the experiment. Figs 14 and 15 show results of Incubation Experiments 1 and 3, respectively. Experiments 2 and 4 are currently undergoing analysis. From these experiments, only the addition of N (Experiment 1, Fig. 14) produced a significant increase in Fo relative to controls. It is notable that in Experiment 1, all treatments, including controls showed a sharp decrease in Fo, which was partially reversed in the +N treatment. All treatments in Experiment 1 also showed reduced ETR relative to controls. In contrast, Experiment 3 showed increases in Fo with little significant difference between controls and nutrient additions.

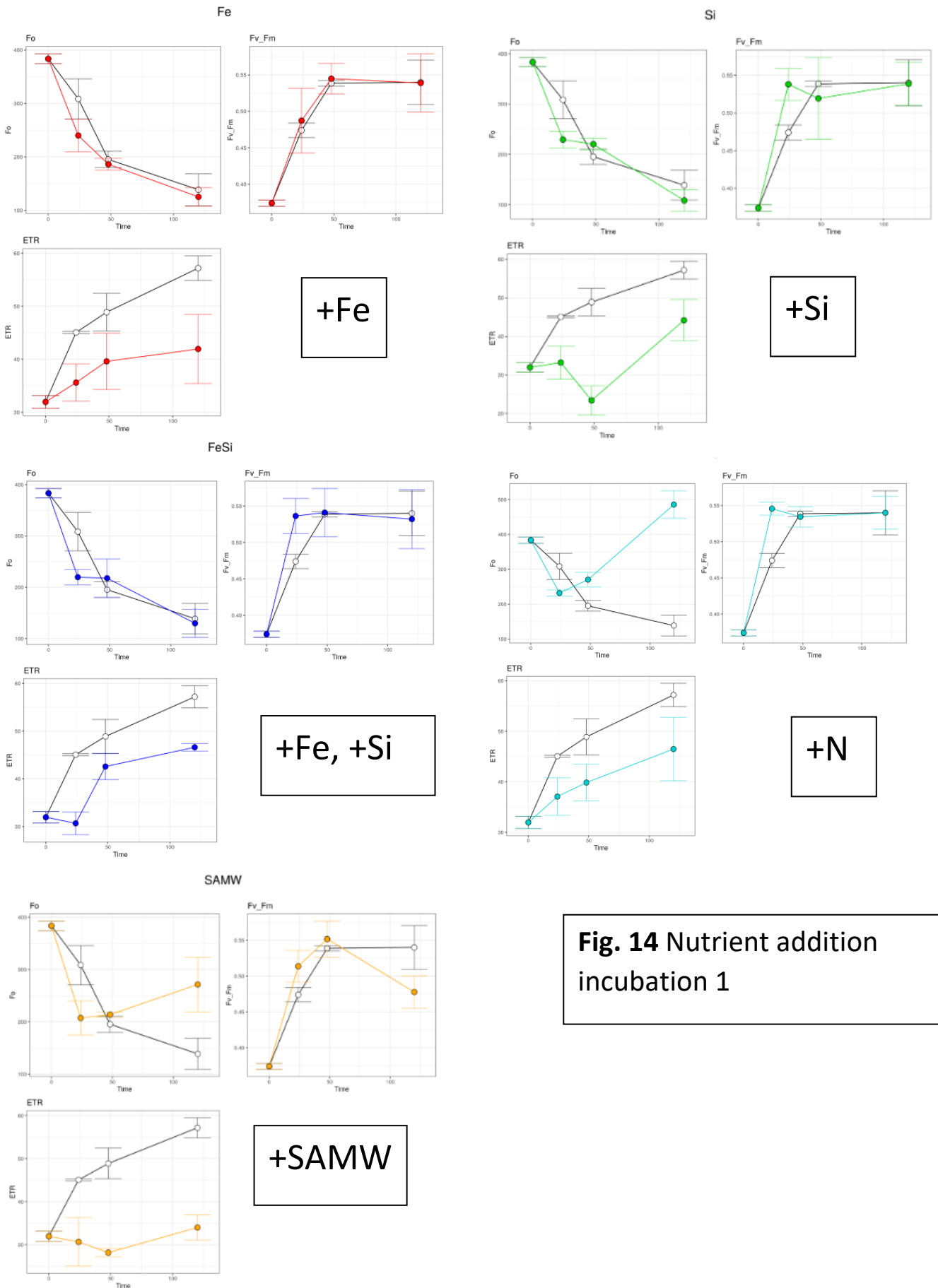


**Fig. 14** Nutrient addition incubation 1

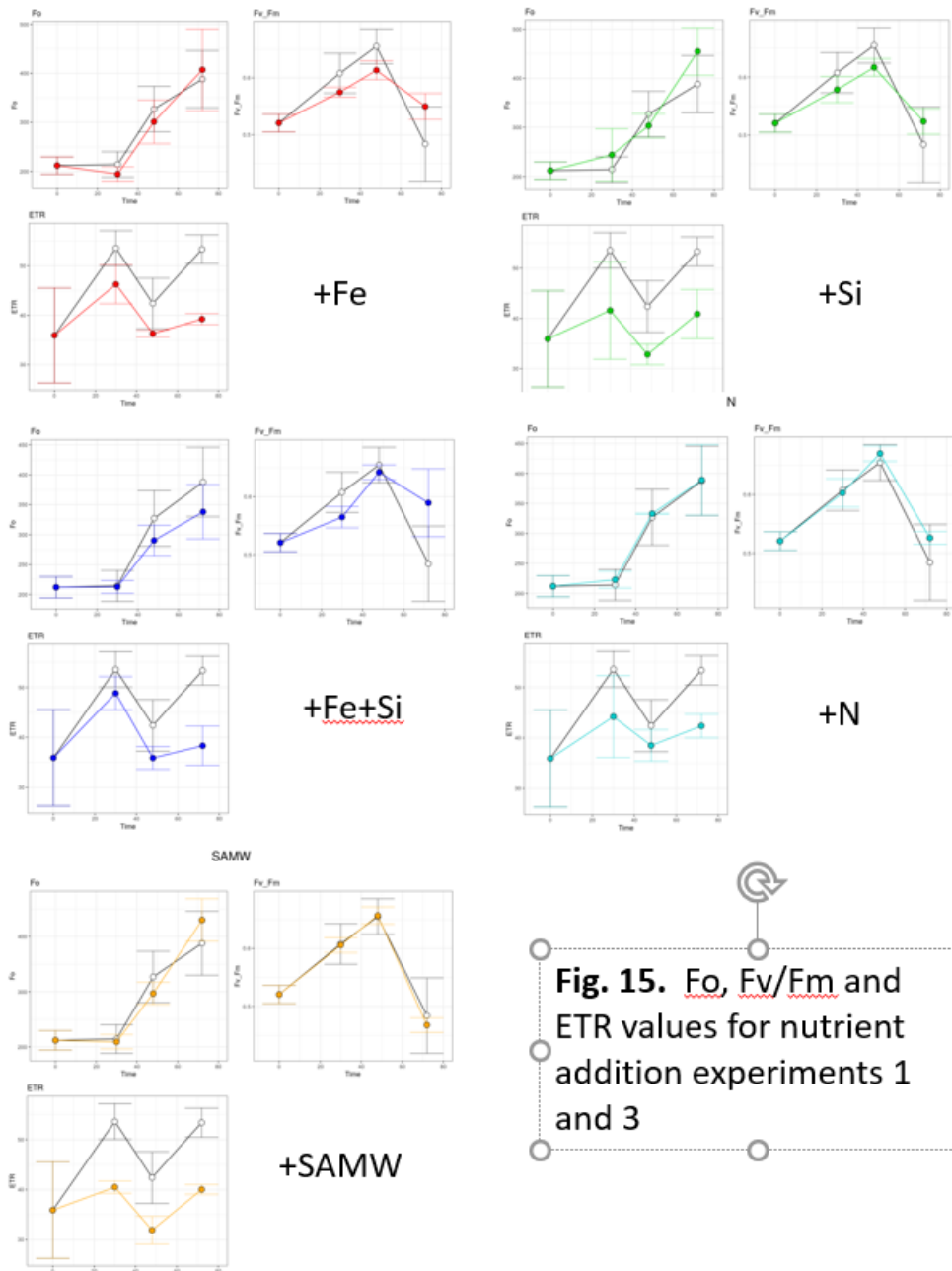


**Fig. 15.** Fo, Fv/Fm and ETR values for nutrient addition experiments 1 and 3

#### **4.5 DNA and RNA**

Samples for DNA and were collected from all DCM and surface CTDs (where chlorophyll fluorescence was significant) and from underway samples that showed sufficiently high chlorophyll or BB' values.

DNA samples will be analysed with high throughput sequencing. RNA samples will provide a resource for probing expression of specific genes and total population transcriptomes.

#### **References**

Murchie EH, Lawson T (2013) Chlorophyll fluorescence analysis: a guide to good practice and understanding some new applications. *J. Exp Bot* 64, 3983-3998.